

Stability Analysis of Static Spherical Spacetime in Extended Symmetric Teleparallel Gravity

M. Zeeshan Gul ^{*}, M. Sharif [†] and Adeeba Arooj [‡]

Department of Mathematics and Statistics, The University of Lahore,
1-KM Defence Road Lahore-54000, Pakistan.

Abstract

Our manuscript aims to analysis the viability and stability of anisotropic stellar objects in the modified symmetric teleparallel gravity. A particular model of this extended theory is considered to formulate explicit field equations which govern the interaction between matter and geometry. The configuration of static spherical symmetric structures is examined through the Finch-Skea solution. However, the values of unknown constants in the metric potentials are evaluated by the Darmois junction conditions. For the viability of proposed stellar objects, the physical parameters including density, pressure, anisotropy, mass, energy constraints, compactness function and redshift are analyzed. Furthermore, stability of the proposed stellar objects is investigated by causality condition, Herrera cracking approach and adiabatic index. Our findings indicate that the proposed stellar objects are viable as well as stable in the presence of correction terms.

Keywords: Modified theory; Stellar objects; Darmois Junction conditions.

PACS: 98.58.M; 04.50.Kd; 97.60.Jd; 98.35.Ac.

^{*}mzeeshangul.math@gmail.com

[†]msharif.math@pu.edu.pk

[‡]aarooj933@gmail.com

1 Introduction

Einstein's gravitational theory (GR) serves as a cornerstone by providing a comprehensive description of gravitational field and matter on cosmic scales. In GR, spacetime is described using mathematical structures defined by the Riemann's metric. This metric encodes information about distance and angles in spacetime which allows physicists to understand the curvature of spacetime caused by gravity. However, Weyl [1] introduced the concept of a *length connection* which is different from the standard metric connection used in Riemannian geometry. Weyl's theory focuses on gauging the conformal factor adjusting the scale of distances. Weyl introduced the concept of non-metricity which assures that divergence of the metric tensor exists. This departure from Riemannian geometry is a new perspective on the geometric nature of spacetime. Non-Riemannian geometries incorporate additional geometric quantities like torsion and non-metricity. Torsion refers to the twisting or rotation of spacetime, while non-metricity involves deviations from the standard concept of distance allowing for a broader understanding of spacetime geometry. Torsion represents gravitational interaction with teleparallel gravity instead of GR [2]. Teleparallel equivalent to GR reformulates gravity not as a result of spacetime curvature but rather through torsion. In this framework, the connection used has zero curvature but non-zero torsion and is still metric-compatible meaning there is no non-metricity. Symmetric teleparallel gravity provides a different perspective on gravity, focusing on non-metricity as the source of gravitational effects in a flat spacetime scenario, i.e., zero curvature and zero torsion [3]. Various extended theories of gravity in different context has been discussed in [4]-[14].

Xu et al [15] introduced $f(Q, T)$ theory by including the trace of energy-momentum tensor in the action of symmetric teleparallel theory. This proposal comprises theoretical implications, compatibility and relevance in cosmology. In recent research, various studies have delved into the implications of modified $f(Q, T)$ gravity. Fajardo [16] emphasized that this modified theory offers alternatives to the standard cosmological model. Arora et al [17] conducted a study where they constrained several free parameters in two distinct $f(Q, T)$ models through various energy conditions. Their analysis shed light on the viability of this theory, paving way for a new approach to understand the dark sector of the universe. Tayde et al [18] explored the feasibility of traversable wormholes through strange matter in $f(Q, T)$ background. Pradhan et al [19] discussed various physical characteristics of

gravastars such as proper length, energy, entropy and surface energy density in this framework and found a stable gravastar model. Bourakadi et al [20] conducted a comprehensive study on the black holes in this gravity. Loo et al [21] investigated $f(Q, T)$ theory with small anisotropy to study the complete cosmic evolution as our universe is not isotropic since the Planck era. Narawade et al [22] studied cosmic accelerated expansion in an extended symmetric teleparallel gravity to understand evolutionary phase of the universe in modified theory. Khurana et al [23] examined that this modified theory presents valuable insights into the late time cosmic acceleration. Shukla et al [24] investigated an isotropic and homogeneous universe model in this framework by examining deceleration parameter.

Viable characteristics of stellar objects endorse significant progress in alternative theories. Ilyas and Ahmad [25] used observational data from various CS candidates to investigate the behavior of static spherical structures in the framework of $f(R)$ gravity. Rej and Bhar [26] employed the Durgapal-IV metric to analyze the physical characteristics of anisotropic static spherical solutions in $f(R, T)$ theory. Their examination confirmed that the obtained results remain in the physically acceptable range. Das [27] delved into stable spherically symmetric stellar configurations in $f(R, G)$ gravity. Malik et al [28] analyzed the charged anisotropic characteristics of CSs using Karmarkar condition in modified Ricci-inverse gravity. Ditta and Tiecheng [29] discussed a comprehensive analysis of the physical properties of CSs in Rastall teleparallel gravity. Sharif and Gul [30] checked the stability of proposed CSs using sound speed method in squared gravity.

Nashed and Capozziello [31] investigated the viable model for neutron stars in $f(R)$ gravity, suggesting intriguing possibilities to understand the gravitational behavior of dense objects. Dey et al [32] explored the viable anisotropic stellar objects employing the Finch-Skea solutions in $f(R, T)$ framework. Rej et al [33] conducted a detailed examination of the charged CSs in the same theoretical framework, unveiling valuable insights into the interplay between charge and gravity in compact stellar systems. Kumar et al [34] investigated crucial insights into the relationship between $f(R, T)$ gravitational theory and the internal dynamics of CSs. Maurya et al [35] used the Karmarkar condition to probe charged relativistic objects in $f(G, T)$ gravity. Shamir and Malik [36] provided valuable insights into the dynamical stability of compact spherical systems in modified framework. Lin and Zhai [37] investigated the influence of effective fluid parameters on the geometry of CSs in the $f(Q, T)$ theory. The geometry of compact stars with different

considerations in $f(Q)$ and $f(Q, T)$ theory has been studied in [38]-[44].

The above literature emphasizes the importance of exploring the viable attributes of CSs in $f(Q, T)$ theory. This paper is organized as follows. In section **2**, we present the field equations of $f(Q, T)$ gravity and evaluate the unknown parameters through the Darmois junction conditions. Section **3** delves into examining different physical quantities to identify the physical characteristics exhibited by the CSs. Section **4** analyzes the equilibrium state and stability of the CSs, providing insights into their dynamic behavior. The findings and implications of our results are given in section **5**.

2 Stellar Objects in $f(Q, T)$ Theory

The main objective of this section is to provide an outline of the process by which the field equations are formulated using the variational principle in modified $f(Q, T)$ theory. This modified theory has gained significant attention due to its potential explanations for various cosmological phenomena. The gravitational action in this framework is altered by the addition of extra terms that are based on non-traditional geometric measures apart from the metric tensor. The motivation behind considering this modified theory lies in the quest for a more comprehensive framework to describe gravity and cosmic phenomenon.

The action of this theory is expressed as [15]

$$I = \frac{1}{2} \int \left[f(Q, T) + 2L_m \right] \sqrt{-g} d^4x, \quad (1)$$

where L_m is Lagrangian of matter. The non-metricity and deformation tensor are defined as

$$\begin{aligned} Q &= -g^{\gamma\eta} (L_{\xi\gamma}^{\lambda} L_{\lambda\eta}^{\xi} - L_{\xi\lambda}^{\lambda} L_{\gamma\eta}^{\xi}), \\ L_{\xi\gamma}^{\lambda} &= -\frac{1}{2} g^{\lambda\varsigma} (\nabla_{\gamma} g_{\xi\varsigma} + \nabla_{\xi} g_{\varsigma\lambda} - \nabla_{\varsigma} g_{\xi\gamma}). \end{aligned} \quad (2)$$

However, the super-potential of this model is as follow

$$P^{\lambda}_{\gamma\eta} = \frac{1}{4} [(Q^{\lambda} - \bar{Q}^{\lambda}) g_{\gamma\eta} - \delta^{\lambda}_{(\gamma} Q_{\eta)}] - \frac{1}{2} L^{\lambda}_{\gamma\eta}, \quad (3)$$

Although, the relation for Q is

$$Q = -Q_{\lambda\gamma\eta} P^{\lambda\gamma\eta} = \frac{1}{4} (Q^{\lambda\eta\xi} Q_{\lambda\eta\xi} - 2Q^{\lambda\eta\xi} Q_{\xi\lambda\eta} + 2Q^{\xi} \bar{Q}_{\xi} - Q^{\xi} Q_{\xi}), \quad (4)$$

where

$$Q_{\lambda\gamma\eta} = \nabla_{\lambda}g_{\gamma\eta} = -\partial g_{\gamma\eta,\lambda} + g_{\eta\xi}\bar{\Gamma}^{\xi}_{\gamma\lambda} + g_{\xi\gamma}\bar{\Gamma}^{\xi}_{\eta\lambda}.$$

The calculation of the above relation (4) and its detailed variation is given in [15]. Variate the action (1) corresponding to $g_{\gamma\eta}$, we have

$$\begin{aligned} T_{\gamma\eta} &= \frac{-2}{\sqrt{-g}}\nabla_{\lambda}(f_Q\sqrt{-g}P^{\lambda}_{\gamma\eta}) - \frac{1}{2}fg_{\gamma\eta} + f_T(T_{\gamma\eta} + \Theta_{\gamma\eta}) \\ &- f_Q(P_{\gamma\lambda\xi}Q_{\eta}{}^{\lambda\xi} - 2Q^{\lambda\xi}_{\gamma}P_{\lambda\xi\eta}), \end{aligned} \quad (5)$$

where f_T and f_Q are the partial derivatives corresponding to T and Q.

Consider a static spherical spacetime as the interior region of stellar objects to examine the geometry of CSs, defined as

$$ds^2 = dt^2e^{\vartheta(r)} - dr^2e^{\varpi(r)} - r^2d\Omega^2, \quad (6)$$

where $d\Omega^2 = d\theta^2 + \sin^2\theta d\phi^2$. The anisotropic matter distribution is given by

$$T_{\gamma\lambda} = U_{\gamma}U_{\lambda}\varrho + V_{\gamma}V_{\lambda}p_r - p_t g_{\gamma\lambda} + U_{\gamma}U_{\lambda}p_t - V_{\gamma}V_{\lambda}p_t, \quad (7)$$

where V_{γ} is 4-vector and U_{γ} is 4-velocity of the fluid. The matter-Lagrangian is important in various cosmic phenomena as it demonstrates the configuration of fluid in spacetime. The particular value of matter-Lagrangian can yields significant insights. The well known used formulation of the matter-Lagrangian in the literature is $L_m = -\frac{p_r + 2p_t}{3}$ [45]. The modified field equations for static spherical spacetime become

$$\begin{aligned} \varrho &= \frac{1}{2r^2e^{\varpi}} \left[2rQ'f_{QQ}(e^{\varpi} - 1) + f_Q((e^{\varpi} - 1)(2 + r\vartheta') + (e^{\varpi} + 1)r\varpi') \right. \\ &\left. + fr^2e^{\varpi} \right] - \frac{1}{3}f_T(3\varrho + p_r + 2p_t), \end{aligned} \quad (8)$$

$$\begin{aligned} p_r &= \frac{-1}{2r^2e^{\varpi}} \left[2rQ'f_{QQ}(e^{\varpi} - 1) + f_Q((e^{\varpi} - 1)(2 + r\vartheta' + r\varpi') - 2r\vartheta') \right. \\ &\left. + fr^2e^{\varpi} \right] + \frac{2}{3}f_T(p_t - p_r), \end{aligned} \quad (9)$$

$$p_t = \frac{-1}{4re^{\varpi}} \left[-2rQ'\vartheta'f_{QQ} + f_Q(2\vartheta'(e^{\varpi} - 2) - r\vartheta'^2 + \varpi'(2e^{\varpi} + r\vartheta')) \right]$$

$$- 2r\vartheta'' + 2fre^\varpi \Big] + \frac{1}{3}f_T(p_r - p_t). \quad (10)$$

The field equations are complicated because of multivariate functions and their derivatives. We take a specific model as [46]

$$f(Q, T) = \alpha Q + \beta T, \quad (11)$$

where α and β are model parameters. This model enhances our ability to explain gravitational interactions and their connection with matter and energy. This model provides more accurate predictions for mysterious components of the universe phenomena through the refining of mathematical framework and introduction of new dynamical mechanisms. Furthermore, this model stands as a pivotal pursuit in theoretical physics, aiming to unravel the fundamental essence of physical phenomena from the smallest to the largest scales. It emerges from the aspiration for a unified framework capable of elegantly encompassing a wide array of phenomena spanning cosmology to particle physics. The resulting field equations becomes

$$\varrho = \frac{\alpha e^{-\varpi}}{12r^2(2\alpha^2 + \beta - 1)} \left[\beta(2r(-\varpi'(r\vartheta' + 2) + 2r\vartheta'' + \vartheta'(r\vartheta' + 4)) - 4e^\varpi + 4) + 3\beta r(\vartheta'(4 - r\varpi' + r\vartheta') + 2r\vartheta'') + 12(\beta - 1)(r\varpi' + e^\varpi - 1) \right], \quad (12)$$

$$p_r = \frac{\alpha e^{-\varpi}}{12r^2(2\beta^2 + \beta - 1)} \left[2\beta(r\varpi'(r\vartheta' + 2) + 2(e^\varpi - 1) - r(2r\vartheta'' + \vartheta'(r\vartheta' + 4))) + 3(r(\beta\varpi'(r\vartheta' + 4) - 2\beta r\vartheta'' - \vartheta'(-4\beta + \beta r\vartheta' + 4)) - 4(\beta - 1) \times (e^\varpi - 1)) \right], \quad (13)$$

$$p_t = \frac{\alpha e^{-\varpi}}{12r^2(2\beta^2 + \beta - 1)} \left[2\beta(r\varpi'(r\vartheta' + 2) + 2(e^\varpi - 1) - r(2r\vartheta'' + \vartheta'(r\vartheta' + 4))) + 3(r(2(\beta - 1)r\vartheta'' - ((\beta - 1)r\vartheta' - 2)(\varpi' - \vartheta'))) + 4\beta(e^\varpi - 1) \right]. \quad (14)$$

Here, the metric functions (ϑ, ϖ) must be finite and non-singular to obtain the singular free spacetime. In this regard, we consider Finch Skea solutions which are considered as the significant tool to find the exact viable

solutions for interior spacetime, defined as [47]

$$e^{\vartheta(r)} = \left(x + \frac{1}{2}yr\sqrt{zr^2}\right)^2, \quad e^{\varpi(r)} = 1 + zr^2, \quad (15)$$

The arbitrary constants are denoted by x , y and z , respectively. We can evaluate the values of unknown constants by Darmois junction conditions. Also, we consider spherically symmetric vacuum solution as the exterior spacetime. The exterior spacetime is given by

$$ds_+^2 = dt^2\aleph - dr^2\aleph^{-1} - r^2d\Omega^2, \quad (16)$$

where $\aleph = \left(1 - \frac{2m}{r}\right)$. The continuity of metric coefficients at the surface boundary ($r = \mathcal{R}$) gives

$$\begin{aligned} g_{tt} &= \left(x + \frac{1}{2}y\mathcal{R}\sqrt{z\mathcal{R}^2}\right)^2 = \aleph, \\ g_{rr} &= 1 + z\mathcal{R}^2 = \aleph^{-1}, \\ g_{tt,r} &= y\mathcal{R}\sqrt{z}\left(x + \frac{1}{2}y\mathcal{R}\sqrt{z\mathcal{R}^2}\right) = \frac{m}{\mathcal{R}^2}. \end{aligned}$$

Solution of these equation gives

$$x = \frac{2\mathcal{R} - 5m}{2\sqrt{\mathcal{R}^2 - 2m\mathcal{R}}}, \quad y = \frac{1}{\mathcal{R}}\sqrt{\frac{m}{2\mathcal{R}}}, \quad z = \frac{2m}{\mathcal{R}^2(\mathcal{R} - 2m)}.$$

These constants are important to comprehend the interior of the CSs. The mass and radius values for the considered stellar objects are presented in Table 1, while the associated constants can be found in Table 2. In the analysis of stellar objects, it is essential to examine the behavior of metric elements to ascertain the smoothness and absence of singularities in the spacetime. The graphical representation depicted in Figure 1 serves as a crucial tool in this evaluation process. It is clear that both metric components display consistent patterns and show an increasing trend. This behavior is significant as it indicates the absence of any abrupt or irregular fluctuations in the spacetime metrics associated with the stellar objects under consideration. Thus, based on the graphical analysis presented in Figure 1, we can assert that the spacetime appears to be smooth and devoid of singularities, meeting the required criteria for our investigation.

Table 1: Values corresponding to input parameters

CSs	m_{\odot}	$\mathcal{R}(km)$
Her X - 1 [48]	0.85 ± 0.15	8.1 ± 0.41
EXO 1785-248 [49]	1.30 ± 0.2	10.10 ± 0.44
SAX J1808.4-3658 [50]	0.9 ± 0.3	7.951 ± 1.0
4U 1820-30 [51]	1.58 ± 0.06	9.1 ± 0.4
Cen X-3 [52]	1.49 ± 0.08	9.178 ± 0.13
SMC X-4 [48]	1.29 ± 0.05	8.831 ± 0.09
PSR J1903+327 [53]	1.667 ± 0.021	9.48 ± 0.03
LMC X-4 [52]	1.04 ± 0.09	8.301 ± 0.2

Table 2: Values of unknown parameters.

CSs	x	y	z
Her X - 1	-0.924111	0.0343333	0.00682713
EXO 1785-248	-0.908173	0.0304946	0.00599414
SAX J1808.4-3658	-0.918476	0.0363264	0.00792193
4U 1820-30	-0.881827	0.0393097	0.0126622
Cen X-3	-0.887784	0.0376881	0.0108966
SMC X-4	-0.89724	0.0371547	0.00969829
PSR J1903+327	-0.880727	0.0379742	0.0119768
LMC X-4	-0.910411	0.0366062	0.00849917

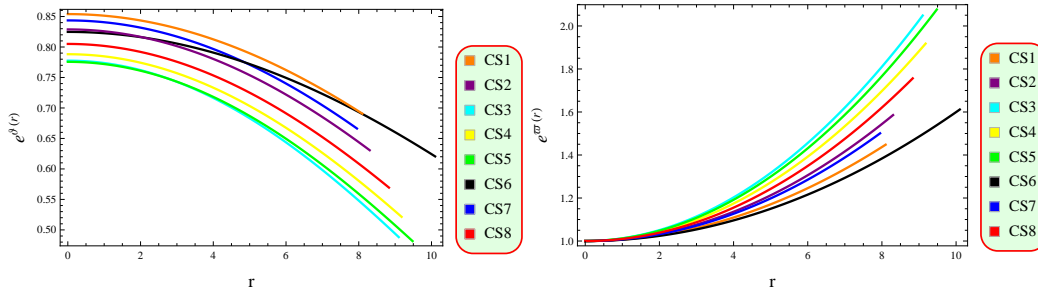


Figure 1: Plot of metric potentials.

3 Viable Characteristics of Stellar Objects

In this section, we examine the viable features of CSs using graphical analysis. For viable and stable CSs with a specific radius, the given conditions are required to be satisfied.

- The metric coefficients need to be monotonically increasing and non-singular at the center, which ensures that spacetimes does not contain any kind of irregularities.
- The behavior of matter contents should be monotonically decreasing and $p_r(r = \mathcal{R}) = 0$ to assure that the CSs has a stable denser core.
- The matter gradient must vanish at the core and then demonstrate negative behavior towards the boundary.
- Positive energy bounds ensure the presence of normal matter in the stellar objects, which is necessary for viable geometry of CSs.
- The EoS parameters must fall in the range of $[0,1]$ for stellar structures to be viable.
- The mass function must be continuous at the core and then shows positively increasing behavior.
- The compactness and redshift functions must be less than $\frac{4}{9}$ and 5.21, respectively, for viable geometry of CSs.
- The forces must satisfy equilibrium condition to maintain the stability.
- For CSs to be stable, the velocities of sound speed should remain in the range of $[0,1]$, while the adiabatic index must be greater than 1.33.

These constraints provide a framework to understand the behavior of CSs and ensure that their properties are consistent.

3.1 Graphical Analysis of Fluid Parameters

The investigation of fluid parameters such as density and pressure is essential to understand the internal features of neutron stars. These matter variables are anticipated to be maximum at the core due to their intense

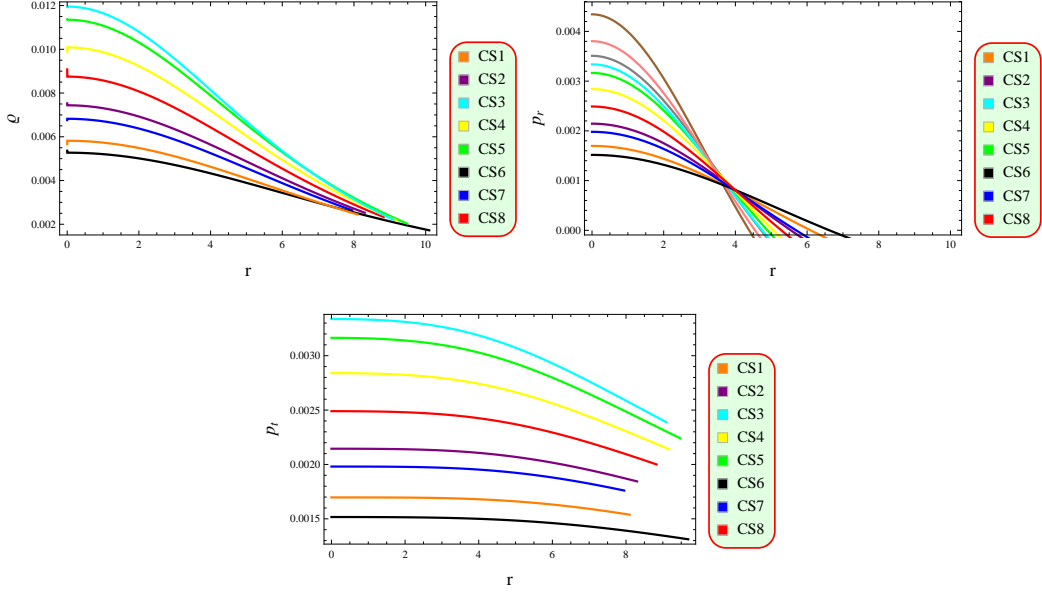


Figure 2: Plot of fluid variables.

density, counteracting gravitational forces and maintaining the stability of CSs against collapse. The corresponding field equations are given as follows

$$\begin{aligned} \rho &= \alpha \left[-3y z r^3 (3 + z r^2) + 2y r (15 + z r^2 (13 + z r^2)) \beta + 2x (3 + z r^2) \sqrt{z r^2} \right. \\ &\quad \left. \times (2\beta - 3) \right] \left[3(1 + z r^2)^2 (y z r^3 + 2x \sqrt{z r^2}) (\beta - 1 + 2\beta^2) \right]^{-1}, \end{aligned} \quad (17)$$

$$\begin{aligned} p_r &= \alpha z \left[2x \sqrt{z r^2} (3 + z r^2 (2\beta - 3) + 6\beta) - y r (6(2 + \beta) + z r^2 (9 - 10\beta + z \right. \\ &\quad \left. \times r^2 (2\beta - 3))) \right] \left[3(1 + z r^2)^2 (y z r^3 + 2x \sqrt{z r^2}) (\beta - 1 + 2\beta^2) \right]^{-1}, \end{aligned} \quad (18)$$

$$\begin{aligned} p_t &= \alpha z \left[2x \sqrt{z r^2} (3 + (6 + 4z r^2) \beta) + y r (-6(2 + \beta) + z r^2 (-3 + (4z r^2 - 2) \right. \\ &\quad \left. \times \beta)) \right] \left[3(1 + z r^2)^2 (y z r^3 + 2x \sqrt{z r^2}) (\beta - 1 + 2\beta^2) \right]^{-1}. \end{aligned} \quad (19)$$

The plots in Figure 2 determine that the matter contents are maximum at the core before decreasing, highlighting the dense nature of the CSs. Additionally, the radial pressure in the considered CSs shows a consistent decrease

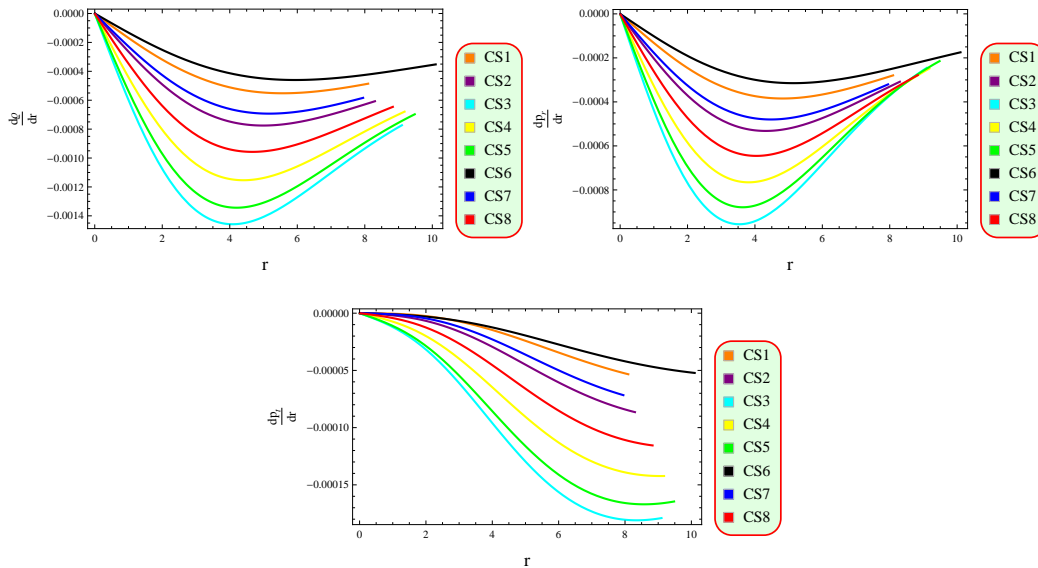


Figure 3: Plot of gradient of fluid variables.

as distance from the center increases until it dissipates at the boundary. Figure 3 manifests that the CSs have highly dense structures in this framework as the gradient of density and pressure components vanish at the core and become negative thereafter.

3.2 Behavior of Anisotropy

An anisotropic fluid refers to a fluid that exhibits different physical properties or behavior in different directions. The term “anisotropic” comes from the Greek words “aniso” meaning unequal or different and “tropos” meaning direction. Anisotropy refers to a difference in pressure along different directions in the system. The pressure in a star is isotropic when there are no additional forces or anisotropic effects present. However, in certain situations such as the presence of strong magnetic fields or other factors, pressure becomes anisotropic. One example of anisotropy is the gravitational field around a rotating object. The gravitational field surrounded by rotating massive objects such as a spinning black hole is not uniform in all directions. The gravitational attraction is stronger in some directions than in others, resulting in anisotropic effects. This phenomenon is known as frame-dragging, where the rotation of the object drags the surrounding spacetime along with

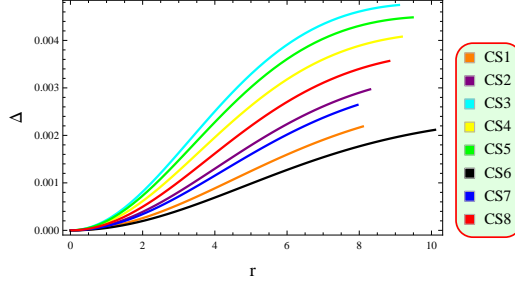


Figure 4: Plot of Anisotropy.

it. Figure 4 indicates the existence of a repulsive force as the behavior of anisotropy is positive, which plays a crucial role in sustaining large-scale structures and preventing gravitational collapse.

3.3 Energy Constraints

Astrophysical entities are composed of a variety of materials in their composition and it is important to differentiate the types of matter (exotic/ordinary) present in the celestial objects. Energy constraints are necessary to examine the viable fluid configurations in the system. These limitations play a crucial role in investigating the presence of specific cosmic formations and understanding how matter and energy interact under the influence of gravity. These constraints manifest the physical viability of the matter configuration in the neutron stars. The energy conditions are characterized into four types as

- Null Energy Condition

$$0 \leq \varrho + p_r, \quad 0 \leq \varrho + p_t.$$

- Dominant Energy Condition

$$0 \leq \varrho \pm p_r \leq 0, \quad 0 \leq \varrho \pm p_t.$$

- Weak Energy Condition

$$0 \leq \varrho + p_r \leq 0, \quad 0 \leq \varrho + p_t, \quad 0 \leq \varrho.$$

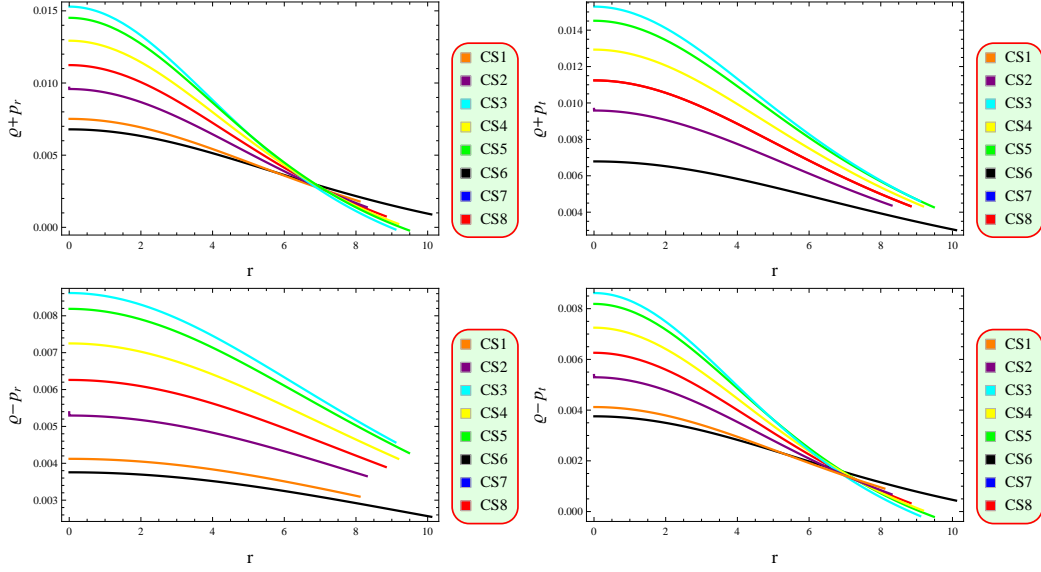


Figure 5: Plot of energy constrains.

- Strong Energy Condition

$$0 \leq \varrho + p_r, \quad 0 \leq \varrho + p_t, \quad 0 \leq \varrho + p_r + 2p_t.$$

Scientists can gain insights into the nature and behavior of cosmic structures by analyzing these energy bounds and their effects on the stress-energy tensor, contributing to our understanding of the dynamics and evolution of the universe. Figure 5 shows that the considered CSs are viable as all energy constraints are satisfied in the presence of modified terms.

3.4 Evolution of State Parameters

The EoS parameters explain how energy density is related to anisotropic pressure in different types of systems. The radial component ($\omega_r = \frac{p_r}{\varrho}$) and transverse component ($\omega_t = \frac{p_t}{\varrho}$) of EoS parameters must satisfy range $[0,1]$ for viable stellar stars [54]. Using Eqs.(17)-(19), we have

$$\omega_r = \left[2x\sqrt{zr^2}(3 + zr^2(3 - 2\beta) + 6\beta) - yr(6(2 + \beta) + zr^2(9 - 10\beta + zr^2(2\beta - 3))) \right] \left[2x\sqrt{zr^2}(3 + zr^2)(2\beta - 3) + y(30r\beta + z^2r^5) \right]$$

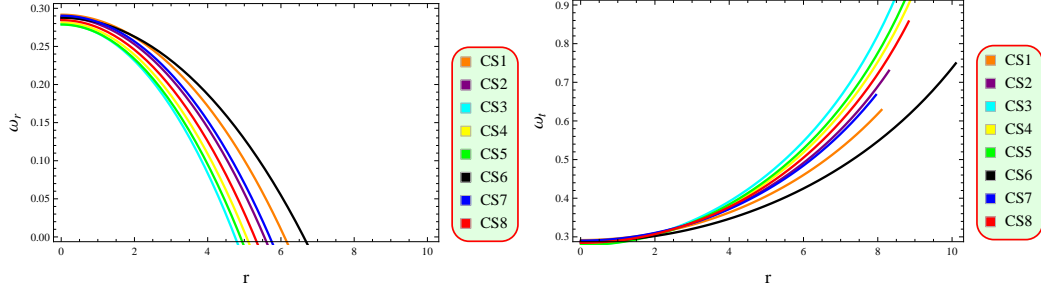


Figure 6: Pots of EoS parameters.

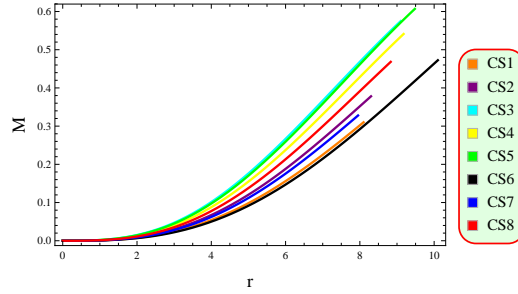


Figure 7: Behavior of mass function.

$$\begin{aligned}
 & \times \left. (2\beta - 3) + zr^3(26\beta - 9) \right]^{-1}, \\
 \omega_t = & \left[2x\sqrt{zr^2}(3 + (6 + 4zr^2)\beta) + yr(-6(2 + \beta) + zr^2(-3 + (4zr^2 \right. \\
 & - 2)\beta)) \right] \left[2x\sqrt{zr^2}(3 + zr^2)(2\beta - 3) + y(30r\beta + z^2r^5(2\beta - 3) \right. \\
 & \left. \left. + zr^3(26\beta - 9)) \right]^{-1}.
 \end{aligned}$$

Figure 6 manifests that the behavior of EoS parameters satisfy the viability condition corresponding to all considered stellar objects.

3.5 Evolution of Different Physical Properties

The mass of stellar objects is described as

$$M = 4\pi \int_0^{\mathcal{R}} r^2 \rho dr.$$

Figure 7 demonstrates that the mass function is monotonically increasing and $M \rightarrow 0$ as $r \rightarrow 0$, suggesting that there are no irregularities in the mass distribution. Various physical characteristics can be assessed to analyze the structural configuration of cosmic objects. A fundamental factor in assessing the viability of CSs is the compactness function, represented by ($u = \frac{M}{r}$). This function offers insights into the distribution of mass relative to the radius of a CS and its concentration. The compactness factor is a physical parameter that provides a quantitative measure of how densely packed mass is within a given radius. There is a specific limit for the compactness function proposed by Buchdhal for a physically relevant model [55]. According to his criterion, the mass-radius ratio should be less than 4/9 for viable stellar objects.

The surface redshift is a significant factor as it provides important information about the brightness and energy of light emitted from their surfaces, which is caused by the gravitational redshift due to the strong gravity. It is a phenomenon which explains the change in frequency (wavelength) of light or other electromagnetic radiations as it travels away from a gravitational field. As the light moves away from the gravitational field, it loses energy and thus its wavelength is increased, causing it to shift towards the red end of the electromagnetic spectrum. It is denoted by Z_s and mathematically expressed as

$$Z_s = -1 + \frac{1}{\sqrt{1 - 2u}}. \quad (20)$$

In case of anisotropic configuration, the redshift at the surface must satisfy the specific condition as $Z_s < 5.211$ for CSs to be viable [56]. The graphs in Figure 8 demonstrate that both compactness and redshift functions meet the essential feasibility criteria.

4 Stability Analysis

It is important to comprehend the behavior and physical characteristics of celestial objects in the field of gravitational physics. The stability of cosmic

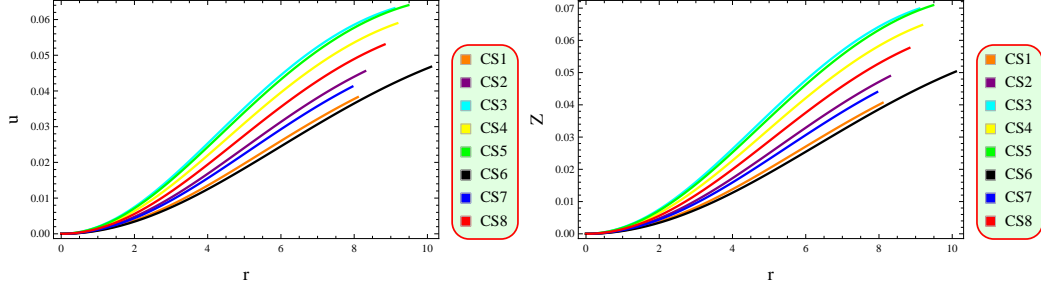


Figure 8: Plot of compactness and redshift functions.

formation is significant to develop their reliability and coherence. Scientists have investigated the conditions that determine the stability of these formations against various forms of oscillations. To assess the stability of pulsars, researchers use the methods such as causality constraint and Herrera cracking approach and adiabatic index provide important perspectives on the structural integrity of astronomical objects.

4.1 Causality Condition

The stability of CSs can be evaluated by considering the causality constraint, which states that nothing can travel faster than the speed of light. In order to maintain stable configurations, both the radial and tangential velocities of sound ($v_r = \frac{dp_r}{d\rho}$ and $v_t = \frac{dp_t}{d\rho}$) must fall in the range of 0 to 1 [57]. These characteristics related to sound speed play a critical role in ensuring the stability of CSs. These are given as follows

$$\begin{aligned}
 v_r &= \left[4x^2 zr(3 + zr^2(3 - 2\beta) + 14\beta) - 4xy\sqrt{zr^2}(6 + 8\beta + zr^2(-16\beta \right. \\
 &\quad \left. + 3 + zr^2(2\beta - 3))) - y^2r(6(2 + \beta) + zr^2(18(2 + \beta) + zr^2(-22\beta \right. \\
 &\quad \left. + 21 + zr^2(2\beta - 3))) \right] \left[4x^2 zr(5 + zr^2)(2\beta - 3) + 4xy\sqrt{zr^2}(20\beta \right. \\
 &\quad \left. + z^2r^4(2\beta - 3) + 5cr^2(-3 + 4\beta)) + y^2r(30\beta + zr^2(90\beta + zr^2(-15 \right. \\
 &\quad \left. + 50\beta + zr^2(2\beta - 3))) \right]^{-1}, \\
 v_t &= 2 \left[4x^2 zr(3 + 2(2 + zr^2)\beta) + 2xy\sqrt{zr^2}(-9 - 2\beta + zr^2(3 + 4
 \end{aligned}$$

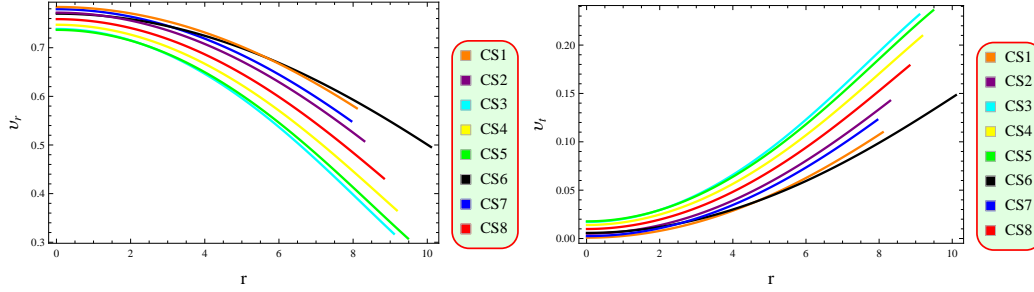


Figure 9: Plot of causality condition.

$$\begin{aligned}
& \times (1 + zr^2)\beta)) + y^2r(-3(2 + \beta) + zr^2(-9(2 + \beta) + zr^2(-3 + 2 \\
& \times (-2 + zr^2)\beta))) \left[4x^2zr(5 + zr^2)(2\beta - 3) + 4xy\sqrt{zr^2}(20\beta + z^2 \right. \\
& \times r^4(2\beta - 3) + 5cr^2(-3 + 4\beta)) + y^2r(30\beta + zr^2(90\beta + zr^2(-15 \\
& \left. + 50\beta + zr^2(2\beta - 3)))) \right]^{-1}.
\end{aligned}$$

Figure 9 shows that the considered CSs satisfy the required condition. Thus, this modified theory supports the existence of physically viable and stable CSs.

4.2 Herrera Cracking Approach

The analysis of solution's stability is based on a mathematical method called the cracking approach ($0 \leq |v_t - v_r| \leq 1$), which was developed by Herrera [58]. Satisfying this condition indicates stable cosmic structures capable of long-term existence, otherwise, it signifies instability and will collapse. This method enables researchers to determine the stability of cosmic structures, which is essential for understanding their behavior in the universe. Figure 10 depicts the fulfillment of the cracking condition as the both radial and tangential sound speed components lie in the range $[0,1]$, which ensures the stability of the stellar objects under consideration.

4.3 Adiabatic Index

This method is considered as a significant method to determine the stability of cosmic objects, providing insights into their composition and behavior.

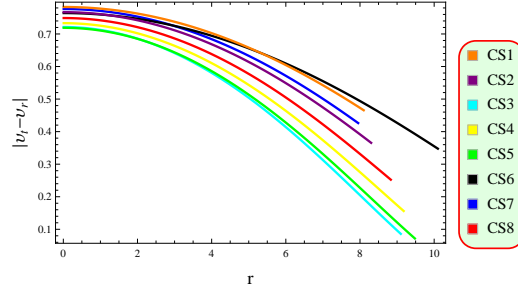


Figure 10: Plot of Herrera cracking approach.

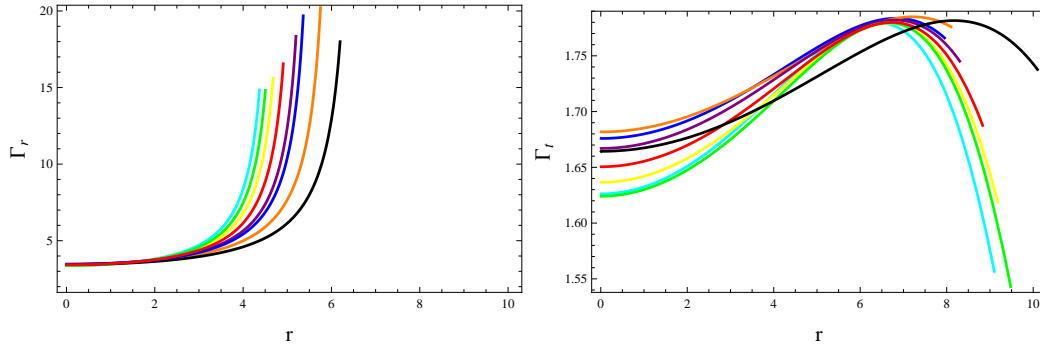


Figure 11: Plot of adiabatic index.

This characterizes how pressure changes corresponding to density variations in stars which plays a pivotal role in astrophysics, described as

$$\Gamma_r = \frac{\varrho + p_r}{p_r} v_r, \quad \Gamma_t = \frac{\varrho + p_t}{p_t} v_t.$$

It is essential to determine the value of Γ for the stability analysis. A stable object exhibits that the values of Γ should be greater than $4/3$, while instability leading to collapse occurs when the value falls below this limit. Figure 11 shows that our system remains stable in the presence of correction terms.

5 Conclusions

This research investigates the feasibility and stability of CSs in the extended symmetric teleparallel theory. The main aim is to investigate whether in-

incorporating non-metricity into the gravitational field equations results in feasible solutions for CSs. Introducing these terms to the theory presents new insights into how matter and geometry interact under extreme gravitational circumstances. Furthermore, we have conducted a graphical analysis of various physical characteristics to verify the viability of the CSs in the proposed theoretical framework. In addition, we have assessed stability through methods that incorporate sound speed and adiabatic index.

The metric functions are essential and have a significant impact in describing the geometry of spacetime. We have found that metric coefficients are consistent and nonsingular which ensure that the spacetime is smooth and devoid of any singularities (Figure 1). This smoothness is a fundamental requirement for any viable cosmological model. The material contents are higher, regular and the most concentrated at the center of the observed CSs (Figure 2) which indicate a stable core and this behavior of fluid parameters is desirable to maintain the structural integrity of the CSs. Furthermore, the decrease in matter content towards the boundary suggests a viable distribution in the CSs. The vanishing radial pressure at the surface boundary ensures the physical viability of the CSs. The matter contents exhibit a negative gradient, indicating a dense profile of the suggested stellar objects (Figure 3).

The anisotropy vanishes at the center of CSs which is a desirable feature for maintaining the stability of the CSs (Figure 4). Moreover, anisotropic pressure is directed outward which is a crucial feature for compact stellar configurations. All energy constraints are positive (Figure 5), which confirm the existence of ordinary matter in the interior of CSs. Figure 6 indicates the viability of the considered model as the EoS parameter lies in the range of 0 and 1. The mass function (Figure 7) remains consistent at the center of the CSs and demonstrates a steady increase as the radial coordinate increases. This behavior is indicative of a viable mass distribution in the CSs. The compactness factor being less than $4/9$ and the redshift being less than 5.2 (Figure 8) support the viability of the compact structures. The stability limits guarantee the existence of stable CSs in this framework (Figures 9-11).

It is worthwhile to mention here that the range of physical quantities in $f(Q, T)$ increases and provides more viable as well as stable compact stars as compared to GR [59]-[61] and other modified theories [62]. For example in $f(R)$ theory, it is found that physical quantities such as effective matter variables, energy conditions, EoS parameters and speed of sound are satisfied

for very small range and the compact star Her X-1 under the effects of the second gravity model does not remain stable [63]. In $f(G, T)$ theory, it is analyzed that the evolution of compact stars (SAXJ1808.4-3658 and 4U1820-30) is supported by all three gravity models while for HerX - 1, there are some restrictions asserted by the second model to be completely physically viable [64]. Additionally, in the framework of $f(R, T^2)$ theory, it is evident that CSs are neither theoretical viable nor stable at the center [65]-[67]. In the light of these findings, we conclude that all the CSs considered in this study exhibit both physical viability and stability at their centers in this modified theory. Consequently, our findings suggest that more viable and stable CSs can exist in this modified framework.

A new class of interior solutions to the Einstein field equations for an anisotropic matter distribution using a linear EoS [68]. They verified the physical acceptability of the solutions by the current estimated data of CS 4U-160852. In contrast, our study diverges by adopting the $f(Q, T)$ theory, a different theoretical framework that allows for a comprehensive exploration of the effects of modified terms on the viability and stability of CSs. Using distinct methodologies and techniques, we have analyzed several anisotropic CSs, discerning their viability and stability under the influence of modified gravitational dynamics. Our findings reveal the feasibility of the proposed CSs even in the presence of modified terms, underscoring the robustness of our theoretical framework. By expanding the scope of our investigation to encompass a broader spectrum of CSs, we contribute to the ongoing discourse on the behavior of CSs in alternative gravitational theory, thus enriching our understanding of astrophysical phenomena across diverse theoretical landscapes.

Data Availability Statement: No data was used for the research described in this paper.

References

- [1] H.S. Weyl, Preuss. Akad. Wiss., **26**:465-478(1918)
- [2] J.B. Jimenez, I. Heisenberg, L.T. Koivisto, Phys. Rev. D, **98**(4):044048(2018)

- [3] R. Aldrovandi, J.G. Pereira, *Teleparallel Gravity: An Introduction* (Springer, 2013)
- [4] A. De Felice, S. Tsujikawa, Living Rev. Relativ., **13**:3(2010); T. Harko, F.S. Lobo, S.I. Nojiri, et al., Phys. Rev. D, **84**(2):024020(2011)
- [5] M. Sharif, M.Z. Gul, Eur. Phys. J. Plus, **133**:1-10(2018)
- [6] M. Sharif, M.Z. Gul, Phys. Scr., **96**(10):105001(2021)
- [7] M. Sharif, M.Z. Gul, Chin. J. Phys., **71**:365-374(2021)
- [8] M.Z. Gul, M. Sharif, S. Shabbir, Eur. Phys. J. C, **84**(8):802(2024)
- [9] M.Z. Gul, M. Sharif, I. Hashim, Phys. Dark Universe, **45**:101537(2024)
- [10] M.Z. Gul, M. Sharif, Phys. Scr., **99**:055036(2024)
- [11] M.Z. Gul, M. Sharif, Chin. J. Phys., **88**:388-405(2024)
- [12] M.Z. Gul, M. Sharif, Phys. Scr., **99**(5):055036(2024)
- [13] M.Z. Gul, M. Sharif, A. Afzal, Chin. J. Phys., **89**:1347-1361(2024)
- [14] M. Sharif, M.Z. Gul, I. Hashim, Phys. Dark Universe, **46**:101606(2024)
- [15] Y. Xu, G. Li, T. Harko, et al., Eur. Phys. J. C, **79**:1-19(2019)
- [16] A. Najera, A. Fajardo, Phys. Dark Universe, **34**:100889(2021)
- [17] S. Arora, J.R.L. Santos, P.K. Sahoo, Phys. Dark Universe, **31**:100790(2021)
- [18] M. Tayde, Z. Hassan, P.K. Sahoo, Phys. Dark Universe, **42**:101288(2023); M. Tayde, J.R. Santos, J.N. Araujo, et al., Eur. Phys. J. Plus, **138**(6):539(2023)
- [19] S. Pradhan, D. Mohanty, P.K. Sahoo, Chin. Phys. C, **47**(9):095104(2023)
- [20] K. El Bourakadi, M. Koussour, G. Otalora, et al., Phys. Dark Universe, **41**:101246(2023)
- [21] T.H. Loo, M. Koussour, A. De, Ann. Phys., **454**:169333(2023)

- [22] S.A. Narawade, M. Koussour, B. Mishra, Nucl. Phys. B, **992**:116233(2023)
- [23] M. Khurana, H. Chaudhary, S. Mumtaz, et al., Phys. Dark Universe, **43**:101408(2024)
- [24] B.K. Shukla, R.K. Tiwari, A. Beesham, et al., Mod. Phys. Lett. A, **39**(05):2450005(2024)
- [25] M. Ilyas, D. Ahmad, Chin. J. Phys., **88**:901-912(2024)
- [26] P. Rej, P. Bhar, New Astron., **105**:102113(2024)
- [27] K.P. Das, U. Debnath, A. Ashraf, Phys. Dark Universe, **43**:101398(2024)
- [28] A. Malik, A. Arif, M.F. Shamir, Eur. Phys. J. Plus, **139**(1):67(2024)
- [29] A. Ditta, X. Tiecheng, Phys. Scr., **99**(2):025012(2024)
- [30] M. Sharif, M.Z. Gul, Fortschr. Phys., **71**(4):2200184(2023)
- [31] G.G. Nashed, S. Capozziello, Eur. Phys. J. C, **81**(5):1-20(2021)
- [32] S. Dey, A. Chanda, B.C. Paul, Eur. Phys. J. Plus, **136**(2):228(2021)
- [33] P. Rej, P. Bhar, M. Govender, Eur. Phys. J. C, **81**(4):316(2021)
- [34] J. Kumar, H.D. Singh, A.K. Prasad, Phys. Dark Universe, **34**:100880(2021)
- [35] S.K. Maurya, K.N. Singh, R. Nag, Chin. J. Phys., **74**:313-327(2021)
- [36] M.F. Shamir, A. Malik, Chin. J. Phys., **69**:312-321(2021)
- [37] R.H. Lin, X.H. Zhai, Phys. Rev. D, **103**(12):124001(2021)
- [38] M. Adeel, M.Z. Gul, S. Rani, et al., Mod. Phys. Lett. A, **38**(34):2350152(2023)
- [39] S. Rani, M. Adeel, M.Z. Gul, et al., Int. J. Geom. Methods Mod. Phys., **21**(1):2450033(2024)
- [40] M.Z. Gul, S. Rani, M. Adeel, Eur. Phys. J. C, **84**(1):8(2024)

- [41] M.Z. Gul, M. Sharif, A. Arooj, Fortschr. Phys., **72**(3):2300221(2024)
- [42] M.Z. Gul, M. Sharif, A. Arooj, Phys. Scr., **99**(4):045006(2024)
- [43] M.Z. Gul, M. Sharif, A. Arooj, Gen. Relativ. Gravit., **56**(4):1-42(2024)
- [44] M.Z. Gul, M. Sharif, A. Arooj, et al., Eur. Phys. J. C, **84**(8):775(2024)
- [45] P.H.R.S. Moraes, P.K. Sahoo, Phys. Rev. D, **97**(2):024007(2018); S.K. Maurya, A. Errehymy, D. Deb, et al., Phys. Rev. D, **100**(4)(2019); M. Rahaman, K.N. Singh, A. Errehymy, et al., Eur. Phys. J. C, **80**(3):272(2020)
- [46] Y. Xu, G. Li, T. Harko, et al., Eur. Phys. J. C, **80**(5):1-22(2020)
- [47] M.R. Finch, J.E.F. Skea, Class. Quantum Grav., **6**(4):467(1989)
- [48] M.K. Abubekerov, E.A. Antokhina, A.M. Cherepashchuk, Astron. Rep., **52**:379-389(2008)
- [49] F. Ozel, T. Guver, D. Psaltis, Astrophys. J., **693**(2):1775(2009)
- [50] P. Elebert, M.T. Reynolds, P.J. Callanan, et al., Mon. Not. R. Astron. Soc., **395**(2):884-894(2009)
- [51] T. Guver, F. Ozel, A. Cabrera-Lavers, et al., Astrophys. J., **712**(2):964(2010)
- [52] M.L. Rawls, J.A. Orosz, J.E. McClintock, et al., Astrophys. J., **730**(1):25(2011)
- [53] P.C.C. Freire, C.G. Bassa, N. Wex, et al., Mon. Not. R. Astron. Soc., **412**(4):2763-2780(2011)
- [54] M.F. Shamir, S. Zia, : Eur. Phys. J. C, **77**:1-12(2017)
- [55] A.H. Buchdahl, Phys. Rev. D, **116**(4):1027(1959)
- [56] B.V. Ivanov, Phys. Rev. D, **65**(10):104011(2002)
- [57] H. Abreu, H. Hernandez, L.A. Nunez, Class. Quantum Grav., **24**(18):4631(2007)

- [58] L. Herrera, Phys. Lett. A, **165**(3):206-210(1992)
- [59] M.K. Gokhroo, A.L. Mehra, Gen. Relativ. Gravit., **26**:75-84(1994)
- [60] D. Deb, S.R. Chowdhury, S. Ray, et al., Ann. Phys., **387**:239-252(2017)
- [61] K.N. Singh, M.H. Murad, N. Pant, Eur. Phys. J. A, **53**:1-9(2017)
- [62] M. Sharif, A. Waseem, Can. J. Phys., **94**(10):1024-1039(2016)
- [63] Z. Yousaf, M. Sharif, M. Ilyas, et al., Eur. Phys. J. C, **77**:1-10(2017)
- [64] M.Z.U.H. Bhatti, M. Sharif, Z. Yousaf, et al., Int. J. Mod. Phys. D, **27**(04):1850044(2018)
- [65] M. Sharif, M.Z. Gul, Phys. Scr., **98**(3):035030(2023)
- [66] M. Sharif, M.Z. Gul, Gen. Relativ. Gravit., **55**(1):10(2023)
- [67] M. Sharif, M.Z. Gul, Phys. Scr., **98**(3):035030(2023)
- [68] S. Das, S. Ray, M. Khlopov, et al., Ann. Phys., **433**:168597(2021)